General Disclaimer

One or more of the Following Statements may affect this Document

- This document has been reproduced from the best copy furnished by the organizational source. It is being released in the interest of making available as much information as possible.

- This document may contain data, which exceeds the sheet parameters. It was furnished in this condition by the organizational source and is the best copy available.

- This document may contain tone-on-tone or color graphs, charts and/or pictures, which have been reproduced in black and white.

- This document is paginated as submitted by the original source.

- Portions of this document are not fully legible due to the historical nature of some of the material. However, it is the best reproduction available from the original submission.

NASA TECHNICAL MEMORANDUM

NASA TM X-73411

NASA TM X-73411

ACOUSTIC LINER OPTIMUM IMPEDANCE FOR SPINNING MODES WITH MODE CUT-OFF RATIO AS THE DESIGN CRITERION

by Edward J. Rice
Lewis Research Center
Cleveland, Ohio 44135

TECHNICAL PAPER to be presented at the
Third Aero-Acoustic Conference
sponsored by the American Institute of
Aeronautics and Astronautics
Palo Alto, California, July 20-23, 1976

ACOUSTIC LINER OPTIMUM IMPEDANCE FOR SPINNING MODES WITH MODE CUT-OFF RATIO AS THE DESIGN CRITERION

by Edward J. Rice, Aerospace Engineer,
National Aeronautics and Space Administration
Lewis Research Center
Cleveland, Ohio 44135

Abstract

The theoretical optimum acoustic impedance for higher order spinning modes was studied in cylindrical ducts with a boundary layer at the outer edge of a uniform flow. All of the propagating modes were considered from highly propagating to nearly cut-off. An interesting observation from the results of the study was that the mode cut-off ratio uniquely determined the optimum wall impedance and maximum possible attenuation for a given boundary layer thickness, Mach number and frequency. For example, the (3, 7) mode (three circumferential lobes - seventh radial) has nearly the same optimum wall resistance and reactance as the (8, 5) mode if both mode cut-off ratios are nearly the same. The implications of this phenomenon are quite important in noise suppressor design. Instead of the acoustic power distribution among all of the propagating modes, only the power distribution as a function of cut-off ratio needs to be known. This should be a simpler in-duct measurement than a complete modal measurement. Also, the far field radiation pattern is a function of modal cut-off ratio, and much needed information for liner design can be obtained from these more easily obtained data. A correlation of the results is provided which allows the optimum acoustic impedance to be calculated over the entire cut-off ratio range for any inlet Mach number, boundary layer thickness, frequency, and acoustic mode.

Introduction

Transverse gradients in the steady flow velocity profile (for example, a boundary layer) of an inlet duct have been shown to have a potentially large effect on the propagation of sound in the duct. This problem has been studied extensively (for example, refs. 1 to 6) and a review of the current literature on the subject was reported in reference 7. However, only recently has much attention been devoted to the notion of maximum attenuation and optimum acoustic impedance for duct modes propagating in ducts with a sheared flow (refs. 8 and 9). Such an optimization procedure appears to be a natural step in the evolution of improved acoustic lining design techniques.

In reference 9 the optimum impedance was presented for a wide range of duct modes propagating in ducts with a sheared steady flow near the duct wall. A correlating equation was also presented which unified the results and provided rapid estimation of the boundary layer refraction effects on liner optimum impedance. However, the results were limited to well-propagating modes (far above cut-off) which have essentially axially propagating wave fronts. The purpose of the work reported in this paper is to extend the results of reference 9 to include all of the propagating modes from well-propagating to near cut-off (where waves travel transverse to the velocity gradients). Sample calculations and a correlation equation valid for any cut-off ratio are presented.

A new acoustic liner design procedure based upon modal cut-off ratio is outlined. Proposed experiments to substantiate this design procedure are outlined.

Symbols

A	complex function of mode cut-off ratio
c	speed of sound, m/sec
D	duct diameter, m
ΔdB	sound attenuation in liner, decibels
F	boundary layer refraction function (see eq. (15))
f	frequency, Hz
I_1	integral function across boundary layer (see eq. (17))
i	$\sqrt{-1}$
J_m	Bessel function of first kind, order m
j	index on summation
k	ω/c, m^{-1}
K	factor in axial wave number (see eqs. (1) and (2))
M_0	axial steady flow Mach number - free stream uniform value
m	spinning mode lobe number (circumferential order)
P	acoustic pressure, N/m^2
p	part of acoustic pressure which is function of radial coordinate (see eqs. (1) and (3))
R	amplitude of eigenvalue α
R_{HW}	hardwall eignevalue
R_{opt}	amplitude of eigenvalue at optimum impedance
r	radial coordinate, m
r_0	circular duct radius, m
t	time, sec
x	axial coordinate, m
y	distance from the wall in the boundary layer, m
$\bar{y}$	nondimensional coordinate in boundary layer (y/δ)
α	complex radial eigenvalue ($\alpha = Re^{i\phi}$)
β	mode cut-off ratio (see eq. (11))
β_{HW}	mode cut-off ratio for hardwall ducts (see eq. (10))
$\bar{\beta}$	dimensionless quantity (see eq. (16))
δ	boundary layer thickness, m
ϵ	dimensionless boundary layer thickness, δ/r_0
ζ	optimum specific acoustic impedance with a boundary layer

ζ_0 optimum specific acoustic impedance with zero boundary layer thickness (slip flow at the wall)

η frequency parameter, fD/c

θ specific acoustic resistance

μ radial mode number

ξ nondimensional radial coordinate, r/r_0

σ attenuation coefficient (see eq. (2))

τ propagation coefficient (see eq. (2))

ϕ angular coordinate, radians

ϕ phase of eigenvalue, degrees

ϕ_A phase of complex function A

χ specific acoustic reactance

ψ_m angle of maximum far-field pressure for a mode

ω circular frequency, rad/sec

Theoretical Model

In this section the propagation theory will be only briefly reviewed. The theory is exactly as presented in reference 9 and only enough will be repeated to establish the necessary nomenclature and provide the groundwork for definitions of optimum impedance and cut-off ratio.

The geometry and steady flow profile considered here are as shown in figure 1. The duct is circular, with no splitter rings or hub. The boundary-layer velocity profile is linear near the wall and has a 1/7 power law dependence outside of this linear region. The steady flow is assumed to be uniform in the central region of the duct outside of the boundary layer.

Solutions are of the form,

$$P = p(r)e^{i\omega t - im\phi - ikKx} \tag{1}$$

where m is the spinning mode lobe number and

$$K = \tau - i\sigma = -i(\sigma + i\tau) \tag{2}$$

is a part of the complex wave number which determines the mode damping through σ and the axial phase velocity through τ. In the central uniform flow region closed form solutions exist for $p(r)$ as,

$$p(r) = Jm\left(\frac{\alpha r}{r_o}\right) \tag{3}$$

These solutions are coupled at the outer edge of the boundary layer to the Runge-Kutta integration necessary in the nonuniform flow region. Finally, using the numerical results at the wall, the wall specific acoustic impedance is calculated from,

$$\zeta = \theta + i\chi = \left.\frac{-i\pi\eta p}{\frac{dp}{d\xi}}\right]_{\xi=1} \tag{4}$$

where

$$\xi = r/r_o \tag{5}$$

and the frequency parameter is defined as,

$$\eta = \frac{\omega r_o}{\pi c} = \frac{fD}{c} \tag{6}$$

The damping and propagation coefficients (σ, τ) are related to the radial eigenvalues (α) by,

$$\sigma + i\tau = \frac{-iM_o + i\sqrt{1-(1-M_o^2)(\alpha/\pi r_o)^2}}{1-M_o^2} \tag{7}$$

Note that the quantities K, σ, τ, and α should all have a double subscript (m,μ) to denote the lobe number and radial mode number under consideration. This subscript has been deleted here for brevity.

Optimum Wall Impedance and Maximum Attenuation

Figure 2 shows a set of equal attenuation (σ) and propagation coefficient (τ) contours on the wall impedance plane which are used as an illustration to define the optimum impedance for a particular mode (m = 7, least attenuated radial). As the damping is increased the constant σ contours are seen to be reduced in size. In the limit as the closed contour shrinks in size, the optimum impedance is reached. If the damping is increased further the σ contours are no longer closed contours in the impedance region just discussed but instead are just off optimum contours for the next higher radial mode. The results reported here thus provide the maximum possible damping for the particular mode under consideration.

The results reported in reference 9 were obtained from plots such as shown in figure 2. The results of this paper were obtained by a computer optimization routine which defined the optimum impedance by

$$\left.\frac{\partial|\zeta|}{\partial\sigma}\right)_\tau \approx \left.\frac{\Delta|\zeta|}{\Delta\sigma}\right)_\tau \to 0 \tag{8}$$

and

$$\left.\frac{\partial|\zeta|}{\partial\tau}\right)_\sigma \approx \left.\frac{\Delta|\zeta|}{\Delta\tau}\right)_\sigma \to 0 \tag{9}$$

at the optimum impedance. The subscripts in equations (7) and (8) indicate the quantity which is held constant. Numerical partial derivatives were required due to the numerical Runge-Kutta integration required in the boundary layer. Other mathematical definitions of the optimum impedance are available (references 10 and 11) but equations (8) and (9) provide an efficient routine for the calculation procedure used here. Except for the use of equations (8) and (9) to define the optimum impedance in the computer search routine, the calculation procedure is exactly as in reference 9.

Mode Cut-Off Ratio

Equation (7) can be used to define the cut-off ratio. This is quite simple for hard-walled ducts where the radial eigenvalue α is real. When the second term in the radical of equation (7) exceeds unity this term contributes to the damping (σ) instead of to the propagation coefficient (τ) and the mode is cut-off. The cut-off ratio can thus be

defined as,

$$\beta_{HW} = \frac{\pi\eta}{\chi_{HW}\sqrt{1-M_o^2}} \qquad (10)$$

where χ_{HW} is the mode eigenvalue for hardwalls. Equation (10) expresses the same cut-off ratio concept as in reference 12. When $\beta_{HW} > 1$ the mode propagates, when $\beta \leq 1$ the mode is cut-off and attenuates.

For soft walls where α is complex ($\alpha = Re^{i\phi}$) the modes always damp and there is no precise cut-off point. Perhaps a minimum acoustic power transfer or group velocity definition might be used but these result in complicated expressions. A simple definition is used here as,

$$\beta = \frac{\pi\eta}{R\sqrt{(1-M_o^2)\cos 2\phi}} \qquad (11)$$

for which when $\beta = 1$ the real part of the radical in equation (7) is zero. This reduces to equation (10) for hardwalls and gives results very similar to equation (10) for soft-walls near the optimum impedance since (for a given mode) $R_{opt} > R_{HW}$ but $\cos 2\phi_{opt} < 1$.

Farfield directivity pattern relation to cut-off ratio. - A useful relationship can be established between the fan far-field directivity pattern and the duct mode cut-off ratio. It has been shown (refs. 13 and 14, for example) that the peak in the far field directivity pattern (occurring at angle ψ_m) is related to the duct mode eigenvalue by,

$$\frac{\omega r_o}{c} \sin \psi_m = \chi_{HW} \qquad (12)$$

For hard walls and zero Mach number, equations (6) and (10) can be used in equation (12) to obtain,

$$\sin \psi_m = \frac{1}{\beta_{HW}} \qquad (13)$$

Thus nearly cut-off modes ($\beta \gtrsim 1$) radiate predominantly at 90 degrees from the inlet axis while well propagating modes (β_{HW} large) radiate nearer to the axis.

Results of Calculations

In this section the main conclusions drawn from this study will be illustrated by means of several sample calculations using the procedures of the previous section. In the next section a correlating equation will be given which allows approximate reproduction of the results without the necessity of these time comsuming complete calculation procedures.

Sample calculations made for the conditions in an inlet suppressor tested with a General Electric TF-34 engine are shown in figure 3. The frequency was chosen at 2890 Hz since this represented the frequency of peak attenuation observed in the experiment. The calculated optimum impedance points are shown as open symbols for the several modes considered. The filled symbol represents the estimated impedance of the liner for the stated conditions.

Three interesting points can be seen from figure 3. First, although there are a multitude of modes represented by the calculated points, all of the optimum impedances lie along a common curve. The position occupied along this common curve will be shown to depend upon mode cut-off ratio. Two coincident points have been singled out in the insert table. The property that these two modes have in common is the cut-off ratio. This dependence upon cut-off ratio will be shown later to be more general than just for these calculation conditions. The second observation from figure 3 is that the impedance optima tend to cluster in the near cut-off range of the cut-off ratio. The density of the modes near cut-off is even greater than appears in figure 3 since many of these modes have not been included in the calculations. Note in the figure symbol legend that the modes have been selected in somewhat of a geometric progression of lobe number. This was also done for the radial mode numbers to reduce the number of calculations required. The third observation to be noted from figure 3 is that the estimated liner impedance of this liner lies nearest the cluster of modes shown to be nearing cut-off. A very crude first approximation might be offered that the impedance of a good performing uniform liner might be near the centroid of the collection of propagating mode optimum impedances. This is only a first approximation since each mode peak attenuation, off optimum performance, and acoustic power weighting might in general be expected to be different. However, if anywhere near an equal power distribution among the modes might be expected, then it is natural that the best liner would be located near the densest cluster of mode optima as shown in figure 3. In reference 13, a fairly convincing argument is made that the modes are present with about equal acoustic power in all of the propagating modes at least for static test installations. Thus the TF-34 data point shown on figure 3 represents about the best reactance value for a uniform liner at this frequency. If the reactance had been more negative (thinner liner), the well propagating modes would have damped better but damping of the near cut-off modes would have been decreased. A thicker liner (less negative) would have damped the nearly cut-off modes more but would have left a higher noise level in the well to moderately cut-on modes.

A better liner than the single section liner of figure 3 might be composed of several sections each aimed at a range of cut-off ratio values. Figure 4 shows the results of sample calculations and proposed multi-section liner impedances for a Lycoming YF-102 inlet assemblage which was designed to attack this range of modes. Three boundary layer thicknesses are shown that approximate the range from the beginning to the end of the proposed acoustic treatment. Several spinning modes were considered; some are labeled to show the range of values. Note that the optimum impedance of well-propagating modes ((1,1) for example) is sensitive to boundary layer thickness while that of the nearly cut-off modes is not (for example the (30,3) mode coincident for all three boundary layer thicknesses). This result would be expected when the direction of the wave fronts with respect to the velocity gradient is considered (cut-off spinning mode wavefront motion is transverse to velocity gradients).

The cylindrical section wall lining impedances are shown on figure 4. The three sections (used one at a time) at $\chi = -1$ are designed to attenuate mainly the modes near cut-off. These would have the largest back cavity depth of the sections shown. The two panels at $\chi = -2$ (intermediate back cavity depth) are designed for the intermediate cut-off ratio modes. The thinnest panel at $\chi = -5$ is used to attenuate the well propagating modes. The three panel approach when used as an assembly may resemble what has been called "phased" or "segmented" treatment. However, the reasoning for these panel selections is quite simple and does not depend upon mode conditioning or reflections, although such mechanisms may possible be present.

In order to reduce the noise at a particular frequency, all of the modes carrying acoustic power must be attenuated. If only the modes near cut-off are attenuated, the well propagating modes would act as a floor below which the noise level could not be reduced. More of the same type of treatment would be inefficient since it does readily attenuate the remaining modes.

The liners designed for the near-cut-off modes should provide quite large acoustic power attenuations mainly toward the sideline. This is expected since equation (13) shows that these modes radiate mainly near 90 degrees. The intermediate mode sections should provide more modest attenuations at intermediate angles, while the well propagating mode liner will provide modest attenuation even nearer to the duct axis.

The results of some additional sample calculations are shown in figures 5 and 6 showing optimum resistance and reactance plotted against mode cut-off ratio. These calculations were made using the conditions in a scale model of a QCSEE (Quiet, Clean, Short-haul Experimental Engine Program) low Mach number inlet. Notice again in these two figures that for constant frequency, Mach number, and boundary layer thickness the cut-off ratio correlates the optimum resistance and reactance for the entire range of propagating modes. Also the boundary layer has a relatively large effect on the optimum impedance for modes well above cutoff but not for the near cut-off modes.

Correlating Equations

A correlating equation was developed in reference 9 which expressed the effect of boundary layer refraction on the optimum wall impedance for spinning modes. This equation was developed starting from the theory of reference 4. This correlating equation was tested in reference 9 only for well propagating modes ($\beta \gg 1$). When the equation was checked against the results of this paper for modes near cut-off ($\beta \gtrsim 1$), the equation did not reproduce the results of the exact calculations. The equation was thus modified as follows to make it valid for modes with any cut-off ratio.

The new correlating equation is,

$$\zeta = \frac{(1+\varepsilon)\zeta_o}{1-iFA\zeta_o} \tag{14}$$

which differs from equation (26) of reference 9 only in that the factor A is inserted in the denominator. The following associated expressions are required to evaluate equation (14).

$$F = \varepsilon\pi\eta\left[1 - \frac{\bar{\beta} I_1}{(\pi\eta)^2}\right] \tag{15}$$

$$\bar{\beta} = (\pi\eta K)^2 + m^2 \tag{16}$$

$$I_1 = \int_0^1 \frac{d\bar{y}}{(1-M_o K \bar{y}^{1/7})^2} \tag{17}$$

The integral I_1 can be estimated by,

$$I_1 \approx 1 + 7\sum_{j=1}^{m} \frac{(j+1)}{(j+7)} (M_o K)^j \tag{18}$$

The optimum wall impedance without a boundary layer (ζ_o) for use in equation (14) can be estimated from the correlating equations given in reference 15. Although the determination of the factor A was empirical it was not completely arbitrary in its position in the equation. Since it was known from reference 9 that equation (14) is valid (without A) for well propagating modes (large cut-off ratio β) it was desirable that $A \to 1$ as $\beta \to \infty$. Also the exact calculations of this paper indicate that the boundary layer has very little refractive effect at cut-off since the wave fronts are traveling transverse to the velocity gradients. Thus it is desirable that $A \to 0$ as $\beta \to 1$ and then $\zeta \to \zeta_0$ ($\varepsilon = \delta/r_0 \ll 1$). In keeping with the arguments just made, it was logical to try and correlate A with cut-off ratio. This was found to produce a very good correlation with only a small dependence on mode number beyond the cut-off ratio dependence.

The factor A in equation (14) can be represented as,

$$A = |A| e^{i\phi_A} \tag{19}$$

with

$$|A| = \frac{\beta^2}{\sqrt{(\beta^2-5.66)^2+3.31\beta^2}} = \frac{\beta^2}{\sqrt{\beta^4-8\beta^2+32}} \tag{20}$$

and

$$\phi_A = \frac{225\beta^2}{\sqrt{(\beta^4-3.6)^2+3\beta^2}} \tag{21}$$

with ϕ_A in degrees. The behavior of the functions $|A|$ and ϕ_A are shown in figure 7. For very small values of β, $|A|$ behaves as $\beta^2/4\sqrt{2}$, it peaks at $\sqrt{2}$ for $\beta = 2\sqrt{2}$, and then falls to unity at large β. The phase, ϕ_A, peaks at 180 degrees for $\beta = \sqrt{2}$ and falls off rapidly ($\propto\beta^2$ and $1/\beta^2$) for cut-off ratios below and above this value. There is a small modal dependence to the value of A for which no attempt was made to accommodate into the correlation. There is thus about a ±10 percent scatter around the mean curves shown in figure 7. The correlation for A represented by equations (16) and (17) and shown in figure 7 were generated by observing optimum impedance calculations for many modes. The lobe numbers included $m = 1$, 7, and 20 with radial mode numbers $\mu = 1$, 2, 5, and

10 for each value of m. The cut-off ratios spanned a range from 0.7 to 8.5. Note that for large β, $|A| \to 1$ and $\phi_A \to 0$. Thus the correlation given in reference 9 remains valid for well propagating modes.

Liner Design Considerations

From the discussion in the preceding sections a cut-off ratio distribution might suffice in place of a modal distribution in at least part of the liner design procedure. The optimum wall impedance was shown in figures 3 to 6 to be determined by the modal cut-off ratio alone rather than by the modal numbers (m and μ). In addition, the cut-off ratio distribution might be estimated by the far-field radiation pattern through equation (13). However, no mention of expected attenuation has yet been made and this damping rate will determine the length of treatment required in any given application. In the following discussion some aspects of attenuation rate will be considered.

From the approximate equations given in reference 16, for moderate to well propagating modes, the sound attenuation can be estimated by,

$$\frac{\Delta dB}{L/D} \approx -\frac{8.7}{\beta} R \sin 2\phi \approx \frac{-43}{\beta} \qquad (22)$$

where an average value of $R \sin 2\phi \approx 5$ was used. The eigenvalue approximations of reference 15 were exercised and the quantity $R \sin 2\phi$ was found to be fairly insensitive to modal lobe and radial mode numbers. With $1 \le m \le 20$ and $1 \le \mu \le 10$ the range of $R \sin 2\phi$ was from about 3 to 5.5. The insensitivity observed was due to the fact that as R increases due to either increasing m or μ, then ϕ decreases almost enough to counterbalance the R increase. If equation (22) were valid at all β values then a quite convenient situation would exist. Not only the optimum wall impedance but also the maximum possible damping (per L/D) would be uniquely determined by cut-off ratio. Unfortunately this is not completely true. Very near cut-off ($\beta \approx 1$) there is an abrupt increase in the modal attenuation for especially the higher order modes which can be seen from figure 5 of reference 16. Again using the results of reference 16 the attenuation at cut-off can be approximated by,

$$\frac{\Delta dB}{L/D} \approx -8.7\sqrt{2}\, R\sqrt{\sin 2\phi} \qquad (23)$$

This equation does not have the compensating effects (as did equation (22)) between R and ϕ. Again for $1 \le m \le 20$ and $1 \le \mu \le 10$, the quantity $R\sqrt{\sin 2\phi}$ varies between 3.5 and 21 and thus equation (23) must be considered as a function of the mode numbers. This modal dependence can probably be ignored as a first estimate at least, since it occurs only very near to cut-off. The damping calculated from equation (22) at $\beta = 1$ will be less than the actual damping from equation (23) so a conservative design should result from this approximation.

Another attenuation consideration must be realized. Any given wall material is optimum only at one modal cut-off ratio. This cut-off ratio may include several modes which would be at their optimum but a multitude of other modes would be off-optimum. The approximate equation technique of reference 15 will be used to handle the off-optimum modes which will allow the rapid estimation of attenuations without the need of the numerical integration required for an exact sound propagation calculation with boundary layers. This approximate equation technique can be cast in terms of cut-off ratio since the only inputs required are the optimum impedance (almost exactly a function of cut-off ratio) and the maximum possible attenuation (approximately a function of cut-off ratio).

One final liner design consideration is offered. Recall that the proposed liners shown in figure 4 were intended to damp the near cut-off, intermediate, and well propagating modes at $\chi = -1$, -2, and -5 respectively for the blade passage frequency only. The $\chi = -1$ is a relatively thick liner while the $\chi = -5$ liner has a quite thin back cavity. An efficient overall liner would have the liner sections compromised somewhat to do double or even triple duty. For example, the $\chi = -5$ liner section could damp well-propagating modes at the blade passage frequency, intermediate modes at the second harmonic and near cut-off modes at the third harmonic frequency.

Concluding Remarks

Sample calculations were presented showing the optimum impedance for a wide range of spinning modes propagating in a cylindrical duct with a sheared flow. Modes were considered from well propagating to cut-off. The key result was that for a given frequency, Mach number, boundary layer thickness, and geometry (which would be normally known inputs) the optimum impedance and maximum possible attenuation are uniquely defined by the modal cut-off ratio as an alternate to actual modes (indices m and μ). Many modes may exist which have the same optimum impedance and damping provided they have the same cut-off ratio. It is suspected that modes of equal cut-off ratio have the same effective angle of incidence on the liner wall.

The results of the calculations were used to generate a correlation equation for the spinning mode optimum wall impedance. This correlation will allow the rapid calculation of optimum impedance in a duct with sheared flow without the numerical integration usually required.

An acoustic liner design procedure was outlined which allows the circumventing of the knowledge of the actual modal distribution. The cut-off ratio distribution can be estimated from far-field directivity patterns and the liner can then be designed at least approximately from this cut-off ratio information. This should be especially useful for liners designed for flight tests where experience is limited and modal measurement may be impractical.

References

1. Pridmore-Brown, D. C., "Sound Propagation in a Fluid Flowing Through an Attenuating Duct," Journal of Fluid Mechanics, Vol. 4, Aug. 1958, pp. 383-406.

2. Mungur, P. and Plumblee, H. E., "Propagation and Attenuation of Sound in a Soft-Walled Annular Duct Containing a Sheared Flow," Basic Aerodynamic Noise Research, SP-207, 1969, NASA pp. 305-327.

3. Ko, S. H., "Sound Attenuation in Acoustically Lined Circular Ducts in the Presence of Uniform Flow and Shear Flow," Journal of Sound and Vibration, Vol. 22, May 1972, pp. 193-210.

4. Eversman, W. and Beckemever, R. J., Transmission of Sound in Ducts with Thin Shear Layers-Convergence to the Uniform Flow Case," The Journal of the Acoustical Society of America, Vol. 52, July 1972, pp. 216-220.

5. Nayfeh, A. H., Kaiser, J. E., and Shaker, B. S., "Effect of Mean-Velocity Profile Shapes on Sound Transmission Through Two-Dimensional Ducts," Journal of Sound and Vibration, Vol. 34, June 1974, pp. 413-423.

6. Yurkovich, R. N., "Attenuation of Acoustic Modes in Circular and Annular Ducts in the Presence of Sheared Flow," AIAA Paper 75-131, 1975, Pasadena, Calif.

7. Nayfeh, A. H., Kaiser, J. E., and Telionis, D. P., "The Acoustics of Aircraft Engine-Duct Systems," AIAA Paper 73-1153, 1973, Montreal, Canada.

8. Schauer, J. J. and Hoffman, E. P., "Optimum Duct Wall Impedance-Shear Sensitivity," AIAA Paper 75-129, 1975, Pasadena, Calif.

9. Rice, E. J., "Spinning Mode Sound Propagation in Ducts with Acoustic Treatment and Sheared Flow," AIAA Paper 75-519, 1975, Hampton, Va.; also NASA TM X-71672.

10. Tester, B. J., "The Optimization of Modal Sound Attenuation in Ducts, in the Absence of Mean Flow," Journal of Sound and Vibration, Vol. 27, Apr. 1973, pp. 477-513.

11. Zorumski, W. E., and Mason, J. P., "Multiple Eigenvalues of Sound-Absorbing Circular and Annular Ducts," Journal of the Acoustical Society of America, Vol. 55, June 1974, pp. 1158-1165.

12. Sofrin, T. G., and McCann, J. F., "Pratt and Whitney Experience in Compressor-Noise Reduction," Preprint 2D2, Nov. 1966, Acoust. Soc. Am., Los Angeles, Calif.

13. Saule, A. V., "Modal Structure Inferred from Static Far-Field Noise Directivity," AIAA Paper 76-574, 1976, Palo Alto, Calif.; also TM X-71709.

14. Homicz, G. F., and Lordi, J. A., "A Note on the Radiative Directivity Patterns of Duct Acoustic Modes," Journal of Sound and Vibration, Vol. 43, Dec. 1975, pp. 283-290.

15. Rice, E. J., "Attenuation of Sound in Ducts with Acoustic Treatment - A Generalized Approximate Equation," TM X-71830, 1975, NASA.

16. Rice, E. J., "Spinning Mode Sound Propagation in Ducts with Acoustic Treatment," 88th Acoustical Society of America Meeting, Nov. 1974, St. Louis, MO; also TM X-71613 and TN D-7913, 1975, NASA.

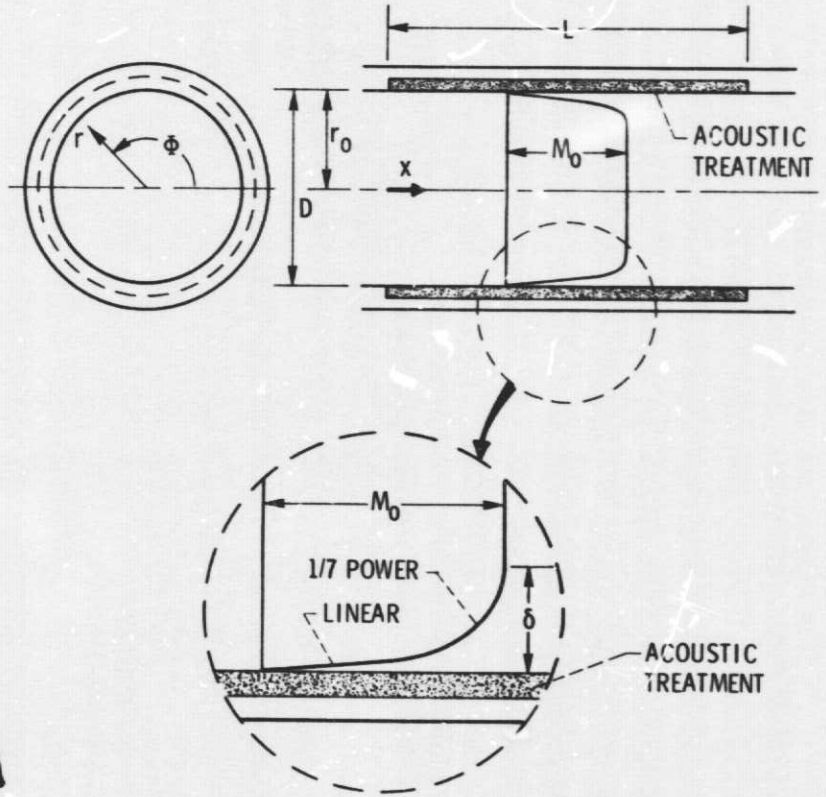

Figure 1. - Geometry and steady-flow velocity profile.

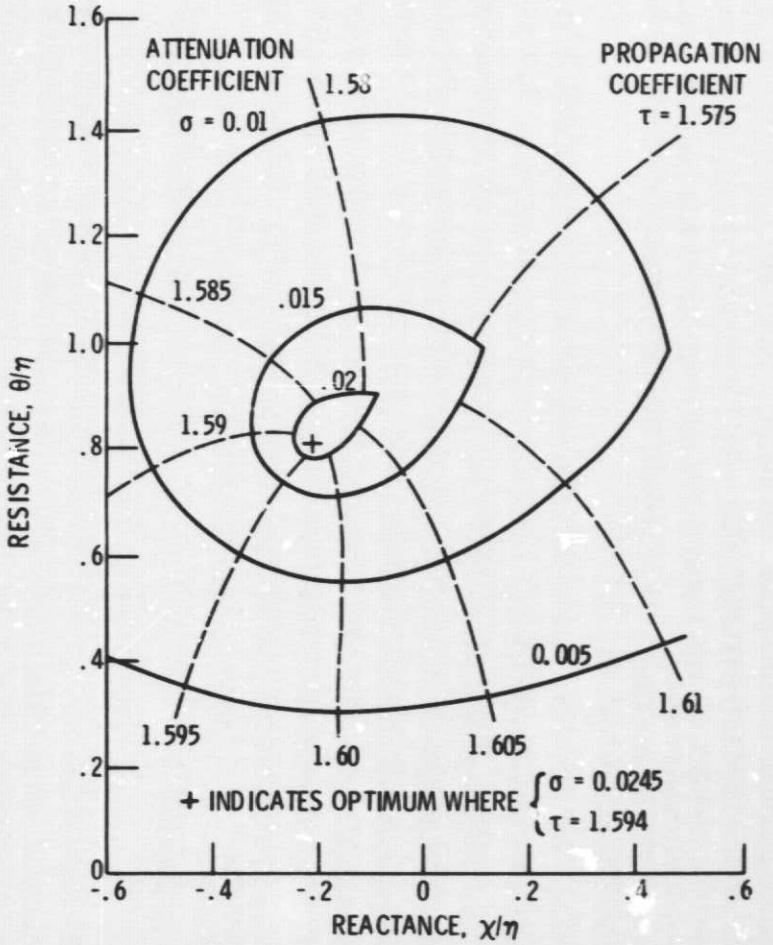

Figure 2. - Constant attenuation and propagation contours for the least attenuated spinning mode using displacement boundary condition. Inlet Mach number, $M_0 = -0.4$; lobe number, m = 7; frequency parameter, $\eta = 10$; boundary layer thickness, $\delta/r_0 = 0$.

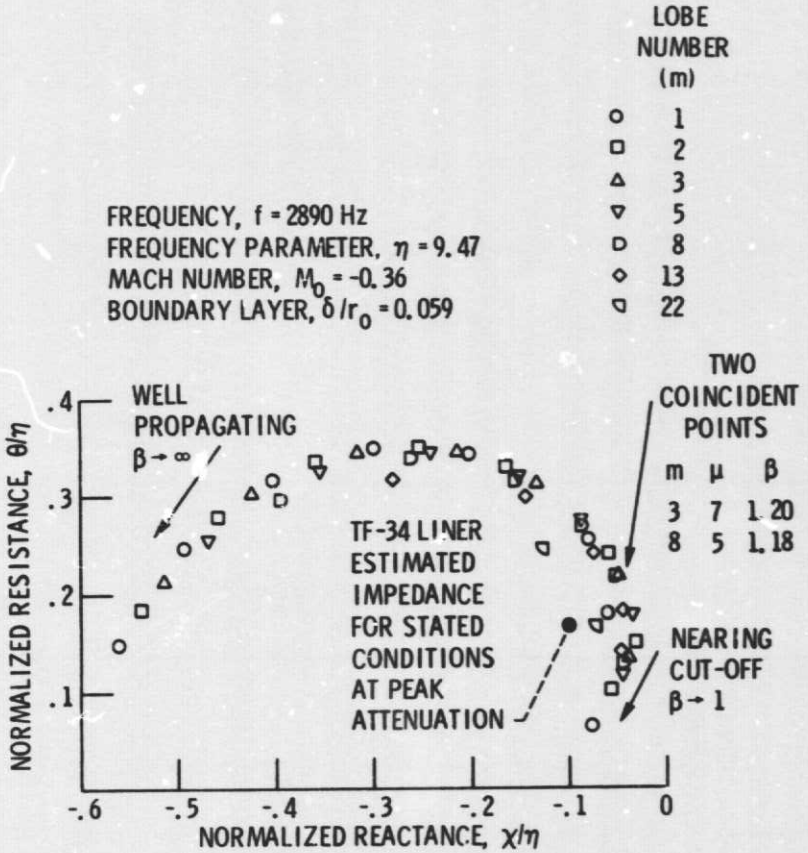

Figure 3. - Example higher order spinning mode optimum impedance locus.

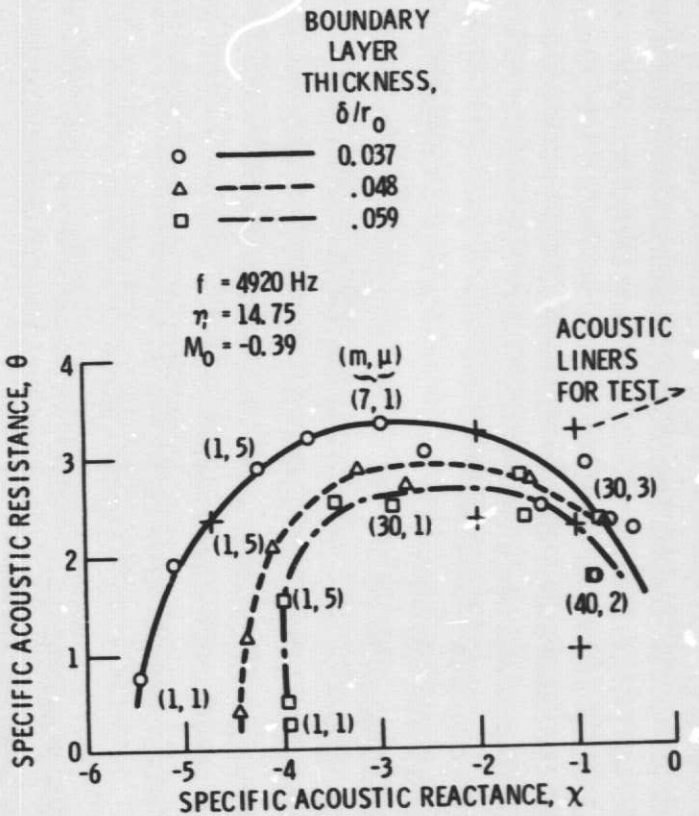

Figure 4. - Liner impedance optima for conditions in the YF 102 inlet, blade passage frequency.

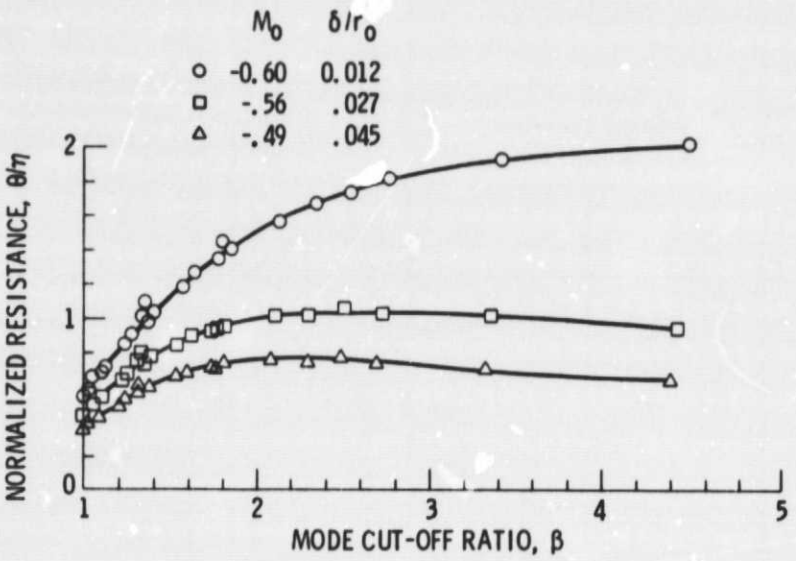

Figure 5. - Optimum liner resistance related to mode cut-off ratio for a QCSEE inlet, frequency 1000 Hz, frequency parameter $\eta = 4.85$.

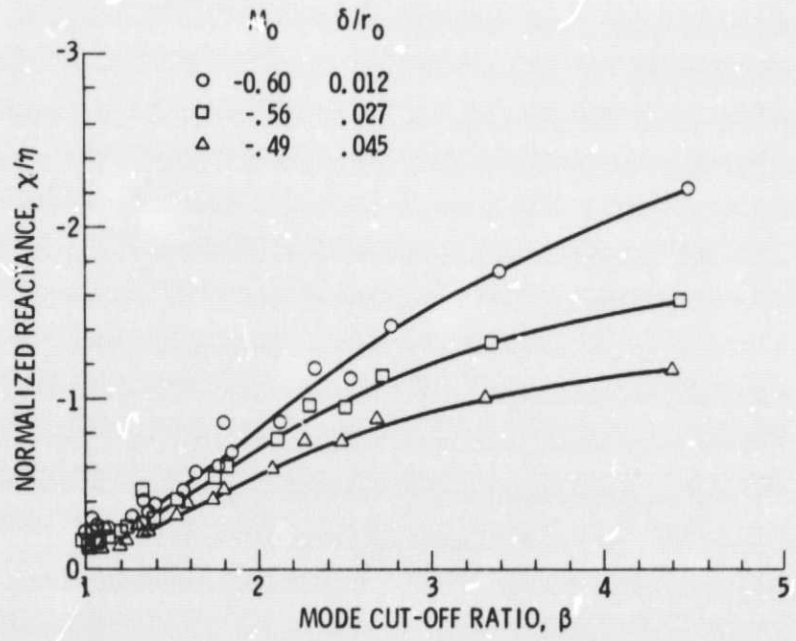

Figure 6. - Optimum liner reactance related to mode cut-off ratio for a QCSEE inlet, frequency 1000 Hz, frequency parameter $\eta = 4.85$.

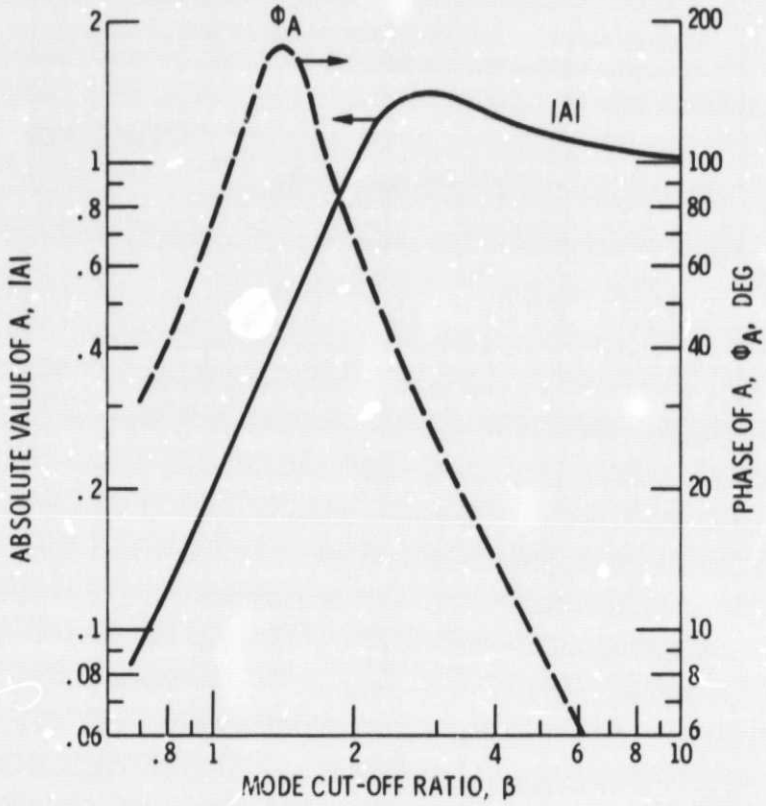

Figure 7. - Amplitude and phase of the cut-off ratio factor, A